Modeling and Numerical Approximation of Traffic Flow Problems

Prof. Dr. Ansgar Jüngel
Universität Mainz
Lecture Notes (preliminary version)

Winter 2002

Contents

1 Introduction

The goal of these lecture notes is to introduce to the modeling of car traffic flow using conservation laws and to the numerical discretization of the resulting hyperbolic differential equations.

Consider the traffic flow of cars on a highway with only one lane (i.e., overtaking is impossible). Instead of modeling the cars individually, we use the *density* $\rho(x,t)$ of cars (in vehicles per kilometer, say) in $x \in \mathbb{R}$ at time $t \geq 0$. The number of cars which are in the interval (x_1, x_2) at time t is

$$\int_{x_1}^{x_2} \rho(x,t)\,dx.$$

Let $v(x,t)$ denote the *velocity* of the cars in x at time t. The number of cars which pass through x at time t (in unit length) is $\rho(x,t)v(x,t)$. We want to derive an equation for the evolution of the car density. The number of cars in the interval (x_1, x_2) changes according to the number of cars which enter or leave this interval (see Figure 1.1):

$$\frac{d}{dt}\int_{x_1}^{x_2} \rho(x,t)\,dx = \rho(x_1,t)v(x_1,t) - \rho(x_2,t)v(x_2,t).$$

Integration of this equation with respect to time and assuming that ρ and v are regular functions yields

$$\begin{aligned}\int_{t_1}^{t_2}\int_{x_1}^{x_2} \partial_t\rho(x,t)\,dx\,dt &= \int_{t_1}^{t_2} \left(\rho(x_1,t)v(x_1,t) - \rho(x_2,t)v(x_2,t)\right)\,dx\,dt \\ &= -\int_{t_1}^{t_2}\int_{x_1}^{x_2} \partial_x\left(\rho(x,t)v(x,t)\right)\,dx\,dt.\end{aligned}$$

Since $x_1, x_2 \in \mathbb{R}$, t_1, $t_2 > 0$ are arbitrary, we conclude

$$\rho_t + (\rho v)_x = 0, \qquad x \in \mathbb{R},\ t > 0. \tag{1.1}$$

This is a partial differential equation. It has to be supplemented by the initial condition

$$\rho(x,0) = \rho_0(x), \qquad x \in \mathbb{R}. \tag{1.2}$$

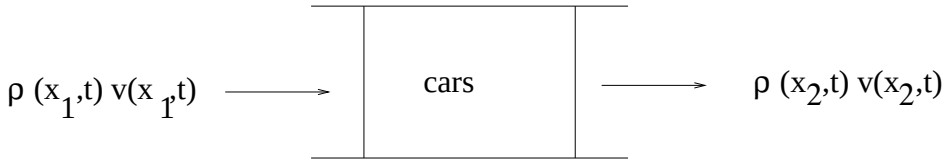

Figure 1.1: Derivation of the conservation law.

We also need an equation for the velocity v. We assume that v only depends on ρ (see Section 3 for other choices). If the highway is empty ($\rho = 0$), we will drive with maximal velocity $v = v_{\max}$; in heavy traffic we will slow down and will stop ($v = 0$) in a tailback where the cars are bumper to bumper ($\rho = \rho_{\max}$). The simplest model is the linear relation

$$v(\rho) = v_{\max}\left(1 - \frac{\rho}{\rho_{\max}}\right), \qquad 0 \le \rho \le \rho_{\max}.$$

Equation (1.1) then becomes

$$\rho_t + \left[v_{\max}\rho\left(1 - \frac{\rho}{\rho_{\max}}\right)\right]_x = 0, \qquad x \in \mathbb{R},\ t > 0. \tag{1.3}$$

This equation is a so-called *conservation law* since it expresses the conservation of the number of cars. Indeed, integrating (1.3) formally over $x \in \mathbb{R}$ gives

$$\frac{d}{dt}\int_{\mathbb{R}} \rho(x,t)\,dx = -\int_{\mathbb{R}} \frac{\partial}{\partial x}\left[v_{\max}\rho(x,t)\left(1-\frac{\rho(x,t)}{\rho_{\max}}\right)\right]\,dx = 0,$$

and thus the number of cars in $\mathbb{R}$ is constant for all $t \geq 0$.

Equation (1.3) belongs to the class of *hyperbolic* equations. We call a system of equations

$$\begin{aligned} \partial_t u + \partial_x f(u) &= 0, \qquad x \in \mathbb{R},\ t > 0, && (1.4)\\ u(x,0) &= u_0(x), \qquad x \in \mathbb{R}, && (1.5) \end{aligned}$$

with $f : \mathbb{R}^m \to \mathbb{R}^m$ *hyperbolic* if and only if for any $u \in \mathbb{R}^m$, $f'(u)$ can be diagonalized and has only real eigenvalues. A function $u : \mathbb{R} \times [0,\infty) \to \mathbb{R}^m$ is called a *classical solution* of (1.4)–(1.5) if $u \in C^1(\mathbb{R}\times(0,\infty)) \cap C^0(\mathbb{R}\times[0,\infty))$ and u solves (1.4)–(1.5) pointwise.

Equation (1.3) can be simplified by bringing it in a dimensionless form. Let L and τ be a typical length and time, respectively, such that $L/\tau = v_{\max}$. Introducing

$$x_s = \frac{x}{L}, \qquad t_s = \frac{t}{\tau}, \qquad u = 1 - \frac{2\rho}{\rho_{\max}},$$

we obtain

$$\partial_t \rho = \frac{1}{\tau}\partial_{t_s}\left[\frac{\rho_{\max}}{2}(1-u)\right] = -\frac{\rho_{\max}}{2\tau}\partial_{t_s}u,$$

$$\partial_x\left[v_{\max}\rho\left(1-\frac{\rho}{\rho_{\max}}\right)\right] = \frac{1}{L}\partial_{x_s}\left[v_{\max}\frac{\rho_{\max}}{2}(1-u)\frac{1}{2}(1+u)\right] = -\frac{\rho_{\max}}{2\tau}\partial_{x_s}\left(\frac{u^2}{2}\right),$$

and hence we can write (1.2)–(1.3) as (with (x,t) instead of (x_s,t_s))

$$\begin{aligned} u_t + \left(\frac{u^2}{2}\right)_x &= 0, \qquad x \in \mathbb{R},\ t > 0, && (1.6)\\ u(x,0) &= u_0(x), \qquad x \in \mathbb{R}, && (1.7) \end{aligned}$$

with $u_0 = 1 - 2\rho_0/\rho_{\max}$. If the highway is empty ($\rho = 0$), we have $u = 1$; in a tailback ($\rho = \rho_{\max}$), $u = -1$ holds. Equation (1.6) is also called the *inviscid Burgers equation*.

In order to see how the solutions of (1.6) may look like, consider the following example. Let

$$u_0(x) = \begin{cases} 1 & : \ x < 0 \\ 1-x & : \ 0 \leq x < 1 \\ 0 & : \ x \geq 1, \end{cases} \qquad (1.8)$$

i.e., there are initially no cars in $x < 0$ and a moderate traffic in $x \geq 1$. What happens for $t > 0$? It is easy to check that

$$u(x,t) = \begin{cases} 1 & : \ x < t \\ \frac{1-t-x}{1-2t} & : \ t \leq x < 1-t \\ 0 & : \ x \geq 1-t \end{cases}$$

is a solution of (1.6)–(1.7) for $x \in \mathbb{R}$, $t < 1/2$ which satisfies (1.4) pointwise except at $x = 1$ and $x = 1 - t$ (see Figure 1.2). The solution becomes discontinuous at $t = 1$.

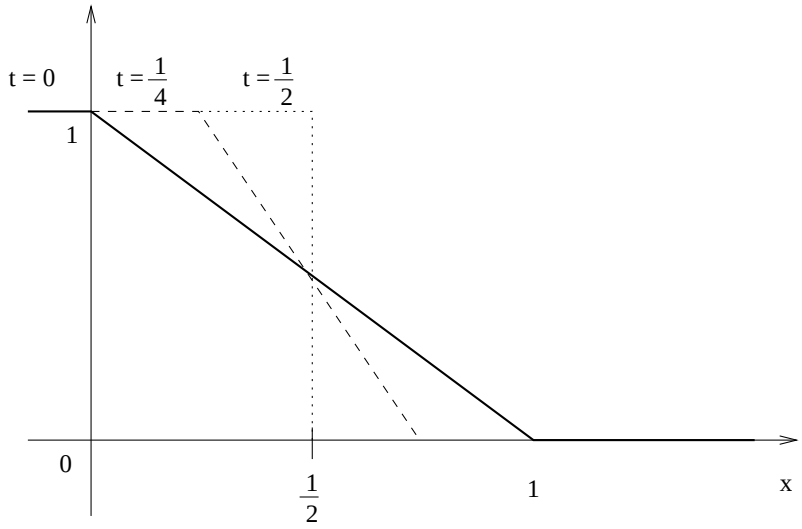

Figure 1.2: Solution of (1.6)–(1.8).

The cars which were initially in $(0, 1)$ drive from the left to the right until no cars were remaining in that interval. As $u = 0$ in $x < 0$, no other cars are coming.

This gives rise to the following questions:

- Does there exist any solution for $t \geq 1/2$?
- If yes, how does the solution for $t \geq 1/2$ look like?
- How can we solve (1.6)–(1.7) for more complicated intial data numerically?

It is clear that we need some theory before we can turn to the numerical treatment of hyperbolic conservation laws.

2 Mathematical theory for scalar conservation laws

In this section we study the problem

$$u_t + f(u)_x = 0, \qquad x \in \mathbb{R},\ t > 0, \tag{2.1}$$

$$u(x, 0) = u_0(x), \qquad x \in \mathbb{R}, \tag{2.2}$$

for some function $f : \mathbb{R} \to \mathbb{R}$. This problem can be solved using the *method of characteristics*.

Definition 2.1 *Let $u : [0, T) \to \mathbb{R}$ be a (classical) solution of (2.1)–(2.2). The solutions χ of the initial-value problem*

$$\chi'(t) = f'(u(\chi(t), t)), \quad t > 0, \qquad \chi(0) = x_0$$

are called the characteristics *of (2.1).*

The main property of the characteristics is that u is constant along them:

$$\frac{d}{dt} u(\chi(t), t) = u_t(\chi(t), t) + u_x(\chi(t), t)\chi'(t) = 0, \qquad t > 0,$$

and hence $u(\chi(t), t) = \text{const.}$ for $t > 0$.

Example 2.2 Let $f(u) = u^2/2$. The characteristics of (2.1) are given as the solutions of

$$\chi'(t) = u(\chi(t), t), \quad t > 0, \qquad \chi(0) = x_0.$$

As $u(\chi(t), t) = \text{const.}$ for $t > 0$, χ is a straight line in the (x, t)-plane through x_0 with slope $1/u_0(\chi(t)) = 1/u_0(x_0)$. Characteristics allow to illustrate the solutions of (1.6)–(1.7) in a compact form. An example with u_0 as in (1.8) is given in Figure 2.1. The characteristics should *not* be confused with the vehicle trajectories; they rather illustrate the "propagation" of the density values. □

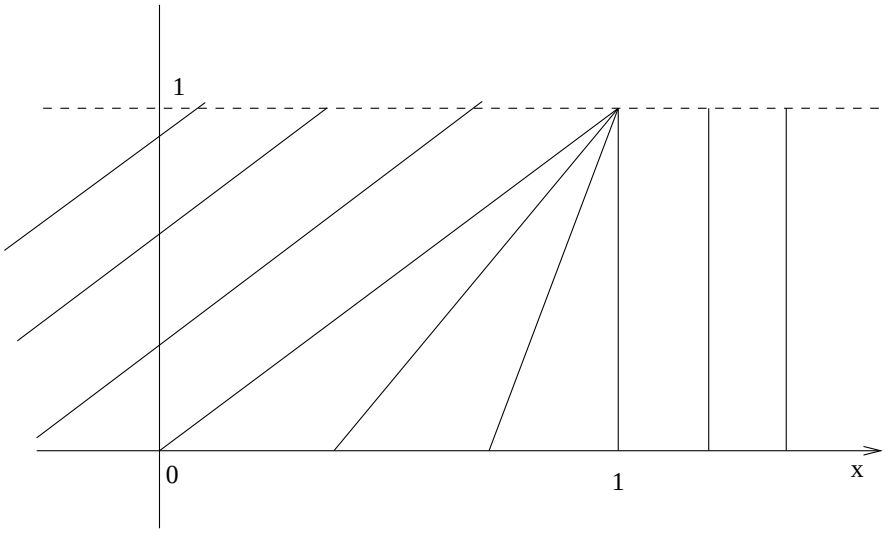

Figure 2.1: Characteristics of (1.6)–(1.8).

Example 2.2 shows again that solutions of (2.1)–(2.2) may develop discontinuities after finite time. Therefore we need a solution concept including discontinuous functions. For

this, let u be a classical solution of (2.1)–(2.2); multiplying (2.1) by $\phi \in C_0^1(\mathbb{R}^2) = \{\phi \in C^1(\mathbb{R}^2) : \phi \text{ has compact support}\}$ and integrating over $\mathbb{R}^2$ yields

$$\begin{aligned} 0 &= \int_0^\infty \int_{\mathbb{R}} (u_t + f(u)_x)\, \phi \, dx\, dt \\ &= -\int_0^\infty \int_{\mathbb{R}} (u\phi_t + f(u)\phi_x)\, dx\, dt - \int_{\mathbb{R}} u(x,0)\phi(x,0)\, dx. \end{aligned}$$

In order to define the last two integrals we only need integrable functions u! This motivates the following definition.

Definition 2.3 *The function $u : \mathbb{R} \times (0,T) \to \mathbb{R}$ is called a* weak solution *of (2.1)–(2.2) if for all $\phi \in C_0^1(\mathbb{R}^2)$*

$$\int_0^\infty \int_{\mathbb{R}} (u\phi_t + f(u)\phi_x)\, dx\, dt = -\int_{\mathbb{R}} u_0(x)\phi(x,0)\, dx.$$

Implicitely, this definition includes some regularity requirements on u (for instance, integrability of u and $f(u)$), but we do not specify them. It is not difficult to check that each classical solution is a weak solution, but the inverse does not need to be true.

Another weak formulation of (2.1) can be obtained as follows. Let u be a classical solution of (2.1)–(2.2). Integrating (2.1) over $(a,b) \times (s,t)$ for any $a, b \in \mathbb{R}$ and $s, t > 0$ gives

$$\int_a^b u(x,t)\, dx - \int_a^b u(x,s)\, dx = -\int_s^t f(u(b,\tau))\, d\tau + \int_s^t f(u(a,\tau))\, d\tau. \tag{2.3}$$

Then we can say that u is a weak solution of (2.1)–(2.2) if $u(\cdot,0) = u_0$ and (2.3) is satisfied for all $a, b \in \mathbb{R}$, $s, t > 0$. It is possible to prove that any weak solution in the sense of Definition 2.3 also satisfies (2.3), but we do not present the (technical) proof.

We now consider conservation laws with special discontinuous initial data.

Definition 2.4 *The problem (2.1)–(2.2) with initial datum*

$$u_0(x) = \begin{cases} u_\ell & : \quad x < 0 \\ u_r & : \quad x \geq 0 \end{cases} \tag{2.4}$$

and u_ℓ, $u_r \in \mathbb{R}$ is called a Riemann problem.

We want to solve the Riemann problem (2.1)–(2.2), (2.4). For this, we observe that with $u(x,t)$ also $u(\alpha x, \alpha t)$ is a solution of (2.1)–(2.2), (2.4) for any $\alpha > 0$. Therefore, u only depends on $\xi = x/t$, i.e. $u = u(\xi)$. This implies

$$0 = u_t + f(u)_x \;=\; -\frac{x}{t^2}u'(\xi) + f'(u(\xi))u'(\xi)\frac{1}{t} = \frac{1}{t}u'(\xi)(f'(u(\xi)) - \xi).$$

Now several possibilities can occur:

- $u'(\xi) = 0 \implies u(\xi) = \text{const.}$
- $f'(u(\xi)) = \xi \implies u(\xi) = (f')^{-1}(\xi)$ (if the inverse of f' exists; a sufficient condition is $f'' > 0$ in $\mathbb{R}$).
- u is discontinuous along $\xi = x/t$, i.e., $u'(\xi)$ does not exist.

This observation motivates to consider three cases:

Case 1: $u_\ell = u_r$. This gives the solution $u(x,t) = u_r = u_\ell$ for all $x \in \mathbb{R}$, $t > 0$.

Case 2: $u_\ell > u_r$. For $f(u) = u^2/2$, a traffic flow interpretation is that the vehicle density in $x > 0$ is larger than in $x < 0$. As the flow direction is from the left to the right, we expect a shock line, i.e. a *discontinuity curve* $x = \psi(t)$. We claim that the discountinuous function

$$u(x,t) = \begin{cases} u_\ell & : \quad x < st \\ u_r & : \quad x \geq st \end{cases} \tag{2.5}$$

is a weak solution of (2.1)–(2.2), (2.4). Then the discontinuity line is given by $x = \psi(t) = st$ and $s = \psi'(t)$ is the *shock speed* which has to be determined. In order to prove our claim let $\phi \in C_0^1(\mathbb{R}^2)$. Then, since $u = \text{const.}$ except on $x = st$,

$$\begin{aligned} \int_0^\infty \int_{\mathbb{R}} u\phi_t \, dx \, dt &= \int_0^\infty \left(\int_{-\infty}^{st} u\phi_t \, dx + \int_{st}^\infty u\phi_t \, dx \right) dt \\ &= \int_0^\infty \Big(\partial_t \int_{-\infty}^{st} u\phi \, dx - s \cdot u(st-0,t)\phi(st,t) \\ &\qquad + \partial_t \int_{st}^\infty u\phi \, dx + s \cdot u(st+0,t)\phi(st,t) \Big) \, dt \\ &= -\int_{\mathbb{R}} u(x,0)\phi(x,0) \, dx - s \cdot (u_\ell - u_r) \int_0^\infty \phi(st,t) \, dt \end{aligned}$$

and, by integration by parts,

$$\begin{aligned} \int_0^\infty \int_{\mathbb{R}} f(u)\phi_x \, dx \, dt &= \int_0^\infty \Big(-\int_{-\infty}^{st} f(u)_x \phi \, dx + f(u(st-0,t))\phi(st,t) \\ &\qquad - \int_{st}^\infty f(u)_x \phi \, dx - f(u(st+0,t))\phi(st,t) \Big) \, dt \\ &= (f(u_\ell) - f(u_r)) \int_0^\infty \phi(st,t) \, dt. \end{aligned}$$

We conclude

$$\begin{aligned} \int_0^\infty \int_{\mathbb{R}} (u\phi_t + f(u)\phi_x) \, dx \, dt &= -\int_{\mathbb{R}} u_0(x)\phi(x,0) \, dx \\ &\qquad - [s \cdot (u_\ell - u_r) - (f(u_\ell) - f(u_r))] \int_0^\infty \phi(st,t) \, dt. \end{aligned}$$

Thus, choosing

$$s = \frac{f(u_\ell) - f(u_r)}{u_\ell - u_r}, \tag{2.6}$$

we have proved the claim.

The choice (2.6) is called the *Rankine-Hugoniot condition*. For a Riemann problem, s is always a constant, i.e., the discontinuity curve is always a straight line. This may not be true for general initial data. In this situation, the Rankine-Hugoniot condition generalizes to [4, Sec. 106]

$$s(t) = \psi'(t) = \frac{f(u_\ell(t)) - f(u_r(t))}{u_\ell(t) - u_r(t)}, \tag{2.7}$$

where

$$u_\ell(t) = \lim_{x \nearrow \psi(t)} u(x,t), \qquad u_r(t) = \lim_{x \searrow \psi(t)} u(x,t). \tag{2.8}$$

It can be shown that (2.5) is the unique weak solution of (2.1)–(2.2) (see Theorem 2.9).

Example 2.5 Let $f(u) = u^2/2$ and $u_\ell = 0$, $u_r = -1$. Then the shock speed is $s = \frac{1}{2}(u_\ell + u_r) = -\frac{1}{2}$, and the solution of (2.1)–(2.2), (2.4) is illustrated in Figure 2.2. The traffic flow interpretation is the following. In $x < st = -t/2$, cars with a moderate density are coming from the left and stop at the tailback at $x = -t/2$. In $x > -t/2$, the density is maximal and the cars are bumper to bumper and are not moving. The shock line $x = -t/2$ denotes the beginning of the tailback. □

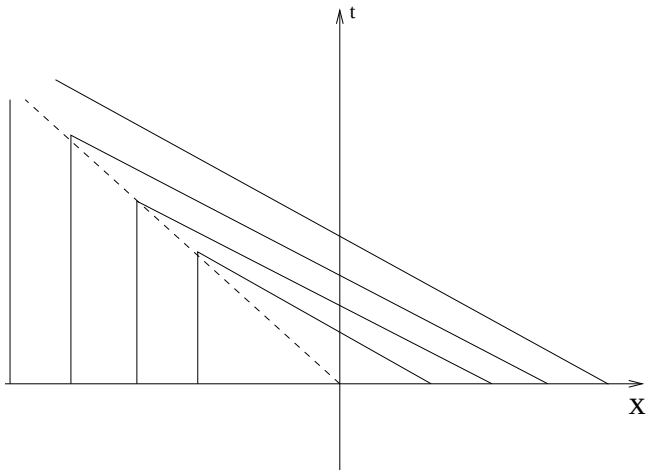

Figure 2.2: Characteristics for (1.6)–(1.7) with $u_\ell = 0$, $u_r = -1$.

Case 3: $u_\ell < u_r$. For this case we assume that $f'' > 0$ in $\mathbb{R}$. One solution is given by (2.5), as the above proof does not need a sign on $u_\ell - u_r$:

$$u_1(x,t) = \begin{cases} u_\ell & : \quad x < st \\ u_r & : \quad x \geq st. \end{cases}$$

It can be shown that also

$$u_2(x,t) = \begin{cases} u_\ell & : \quad x < f'(u_\ell)t \\ (f')^{-1}(x/t) & : \quad f'(u_\ell)t \leq x \leq f'(u_r)t \\ u_r & : \quad x > f'(u_r)t \end{cases}$$

is a weak solution (motivated by the computation before Case 1; see Figure 2.3). In fact, it is possible to show that the problem (2.1)–(2.2), (2.4) possesses infinitely many weak solutions! (See, for instance, [5, Sec. 3.5].) What is the physically relevant solution? We present two approaches.

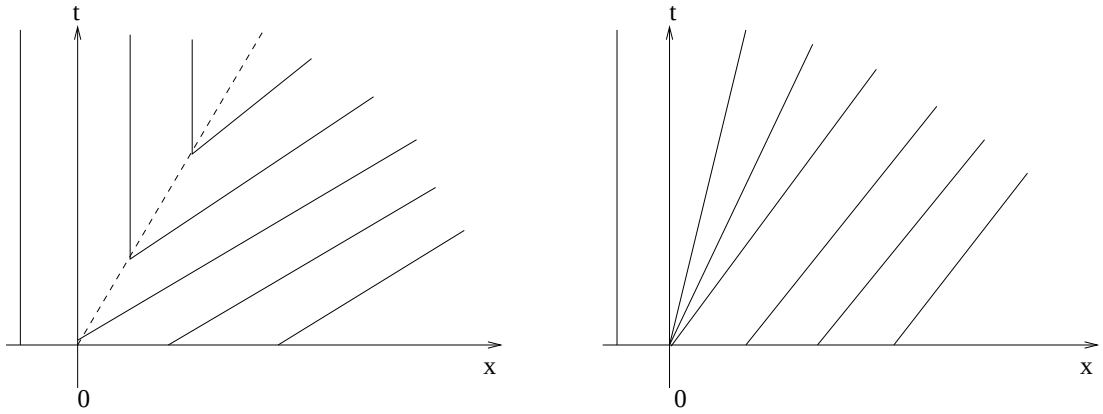

Figure 2.3: Characteristics for (2.1)–(2.2), (2.4) with $f(u) = u^2/2$ and $u_\ell = 0$, $u_r = 1$, corresponding to u_1 (left) and u_2 (right).

In the traffic flow interpretation, the condition $u_\ell < u_r$ means that there are more cars (per kilometer) in $\{x < 0\}$ than in $\{x > 0\}$. The solution u_1 would mean that all cars in $\{x < st\}$ drive with the same velocity $v(u_\ell) = v_{\max}(1 + u_\ell)/2$, whereas all drivers in $\{x > st\}$ move with the velocity $v(u_r) > v(u_\ell)$, and there is a shock at $x = st$. It would be more realistic if the drivers just before the shock line ($x < 0$) tried to drive as fast as the drivers behind the shock ($x > 0$). After some time there are drivers with velocities $v(u_\ell)$ and $v(u_r)$ far away from $x = 0$ and some drivers with velocities between $v(u_\ell)$ and $v(u_r)$ near $x = 0$. Thus, u_2 seems to be the preferable physical solution. The solution u_2 is called *rarefaction wave*.

Is it possible to formulate a general principle which allows to select the physically correct solution? The answer is yes and this leads to the notion of *entropy condition*.

Definition 2.6 *A weak solution $u : \mathbb{R} \times (0,T) \to \mathbb{R}$ of (2.1)–(2.2), (2.4) satisfies the* entropy condition of Oleinik *if and only if along each discontinuity curve $x = \psi(t)$,*

$$\frac{f(u_\ell(t)) - f(v)}{u_\ell(t) - v} \geq \psi'(t) \geq \frac{f(u_r(t)) - f(v)}{u_r(t) - v} \tag{2.9}$$

for all $t \in (0,T)$ and for all v between $u_\ell(t)$ and $u_r(t)$, where $u_\ell(t)$, $u_r(t)$ are defined in (2.8).

Does u_1 satisfy the entropy condition (2.9)? Since

$$\psi'(t) = s(t) = \frac{f(u_r) - f(u_\ell)}{u_r - u_\ell}$$

and f is assumed to be strictly convex, we obtain for any $u_\ell < v < u_r$

$$\frac{f(u_\ell) - f(v)}{u_\ell - v} < \frac{f(u_\ell) - f(u_r)}{u_\ell - u_r} = s < \frac{f(u_r) - f(v)}{u_r - v},$$

which contradicts (2.9). Thus, u_1 does *not* satisfy the entropy condition (2.9). The function u of Case 2, defined in (2.5), however, satisfies (2.9) (if f is convex). As the function u_2 is continuous, we do not need to check (2.9) for this function.

The second approach uses the notion of *entropy*. We call a function $\eta \in C^2(\mathbb{R})$ an *entropy* and $\psi \in C^1(\mathbb{R})$ an *entropy flux* if and only if η is strictly convex and if for any classical solution u of (2.1)–(2.2) it holds

$$\eta(u)_t + \psi(u)_x = 0, \qquad x \in \mathbb{R},\ t > 0. \tag{2.10}$$

The idea of the second approach is to consider the conservation law as an idealization of a diffusive problem given by the equation

$$u_t + f(u)_x = \varepsilon u_{xx}, \qquad x \in \mathbb{R},\ t > 0, \tag{2.11}$$

where $\varepsilon > 0$ is the diffusion coefficient. This equation, together with the initial condition (2.2) has a unique smooth solution u_ε (by the theory of parabolic differential equations), and we assume that

$$\begin{aligned} &u_\varepsilon \to u \quad \text{pointwise in } \mathbb{R} \times (0,T) \text{ for } \varepsilon \to 0, \\ &\|\eta'(u_\varepsilon) u_{\varepsilon,x}\|_{L^1(\mathbb{R}\times(0,T))} \leq c, \end{aligned} \tag{2.12}$$

where the constant $c > 0$ is independent of ε. The limit $\varepsilon \to 0$ is called the *vanishing viscosity* limit. It is possible to prove that u is a solution of (2.1)–(2.2), and we say that u is the physically relevant solution.

Then something happens with the entropy equation (2.10). We multiply (2.11) by $\eta'(u_\varepsilon)$ and choose $\psi' = f' \cdot \eta'$:

$$\eta(u_\varepsilon)_t + \psi(u_\varepsilon)_x = \varepsilon \eta'(u_\varepsilon) u_{\varepsilon,xx} = \varepsilon(\eta'(u_\varepsilon) u_{\varepsilon,x})_x - \varepsilon \eta''(u_\varepsilon) u_{\varepsilon,x}^2.$$

Multiplying this equation by $\phi \in C_0^1(\mathbb{R}\times\mathbb{R})$, $\phi \ge 0$, and integrating over $\mathbb{R}\times(0,\infty)$ gives:

$$\begin{aligned}
&\int_0^\infty \int_{\mathbb{R}} (\eta(u_\varepsilon)_t + \psi(u_\varepsilon)_x)\,\phi\,dx\,dt \\
&= -\varepsilon \int_0^\infty \int_{\mathbb{R}} \eta'(u_\varepsilon) u_{\varepsilon,x}\,\phi_x\,dx\,dt - \varepsilon \int_0^\infty \int_{\mathbb{R}} \eta''(u_\varepsilon) u_{\varepsilon,x}^2\,\phi\,dx\,dt \\
&\le \varepsilon \|\eta'(u_\varepsilon) u_{\varepsilon,x}\|_{L^1(\mathbb{R}\times(0,\infty))}\ \|\phi_x\|_{L^\infty(\mathbb{R}\times(0,\infty))} \\
&\to 0 \qquad (\text{as } \varepsilon \to 0),
\end{aligned}$$

using $\eta''(u_\varepsilon) > 0$ and (2.12). As ϕ is arbitrary, we deduce the *entropy inequality*

$$\eta(u)_t + \psi(u)_x \le 0.$$

Clearly, this only holds for smooth solutions. From the definition of weak solutions follows that the entropy inequality for *weak* solutions writes

$$\int_0^\infty \int_{\mathbb{R}} (\eta(u)\,\phi_t + \psi(u)\,\phi_x) dx\,dt \ge -\int_{\mathbb{R}} \eta(u_0(x))\phi(x,0)\,dx \quad \forall\,\phi \in C_0^1(\mathbb{R}^2). \tag{2.13}$$

We define:

Definition 2.7 *Let $u : \mathbb{R}\times(0,T) \to \mathbb{R}$ be a weak solution of (2.1)–(2.2). Then u is called an* entropy solution *if and only if for all convex entropies η and corresponding entropy fluxes ψ, the inequality (2.13) holds.*

The function u_2 satisfies the entropy equation (2.10) almost everywhere since u_2 is continuous and we can define the derivatives in a weak sense (it is also possible to prove (2.10) in the weak form similarly to (2.13)). Thus, u_2 is an entropy solution. Does this also hold for u_1? We give the (negative) answer in the following example.

Example 2.8 Let $f(u) = u^2/2$, $\eta(u) = u^2$ (hence, $\psi(u) = (2/3)u^3$), and let $\phi \in C_0^1(\mathbb{R}^2)$, $\phi \ge 0$. Then, since $s = (u_\ell + u_r)/2$,

$$\begin{aligned}
&\int_0^\infty \int_{\mathbb{R}} (u_1^2\phi_t + \frac{2}{3}u_1^3\phi_x) dx\,dt \\
&= \int_0^\infty \Big(\partial_t \int_{-\infty}^{st} u_1^2\phi\,dx - s u_\ell^2 \phi(st,t) + \partial_t \int_{st}^\infty u_1^2\phi\,dx + s u_r^2\phi(st,t) \\
&\quad + \frac{2}{3}u_\ell^3\phi(st,t) - \frac{2}{3}u_r^3\phi(st,t)\Big)\,dt \\
&= -\int_{\mathbb{R}} u_0(x)^2\phi(x,0)\,dx - \frac{1}{2}(u_\ell + u_r)(u_\ell^2 - u_r^2)\int_0^\infty \phi(st,t)\,dt \\
&\quad + \frac{2}{3}(u_\ell^3 - u_r^3)\int_0^\infty \phi(st,t)\,dt \\
&= -\int_{\mathbb{R}} u_0(x)^2\phi(x,0)\,dx + \frac{1}{6}(u_\ell - u_r)^3 \int_0^\infty \phi(st,t)\,dt \\
&\ge -\int_{\mathbb{R}} \eta(u_0(x))\phi(x,0)\,dx
\end{aligned}$$

if and only if $u_\ell \geq u_r$. Thus, u_1 is *not* an entropy solution. $\square$

Example 2.8 shows that the two equations

$$u_t + \left(\frac{u^2}{2}\right)_x = 0 \qquad \text{and} \qquad (u^2)_t + \frac{2}{3}(u^3)_x = 0$$

are equivalent *only* for classical solutions.

The above considerations motivate that only rarefaction waves u_2 are the physically relevant solutions of the Riemann problem (2.1)–(2.2), (2.4) if $u_\ell < u_r$. For $u_\ell > u_r$ we have to expect discontinuous solutions with shocks. We summarize the above results in the following theorem.

Theorem 2.9 *Let $f \in C^2(\mathbb{R})$ with $f'' > 0$ in $\mathbb{R}$.*

(1) Let $u_\ell > u_r$ and set $s = (f(u_\ell) - f(u_r))/(u_\ell - u_r)$. Then

$$u(x,t) = \begin{cases} u_\ell & : \quad x < st \\ u_r & : \quad x > st \end{cases}$$

is a weak solution of (2.1)–(2.2), (2.4) satisfying the entropy condition (2.9) of Oleinik.

(2) Let $u_\ell < u_r$. Then

$$u(x,t) = \begin{cases} u_\ell & : \quad x < f'(u_\ell)t \\ (f')^{-1}(x/t) & : \quad f'(u_\ell)t \leq x \leq f'(u_r)t \\ u_r & : \quad x > f'(u_r)t \end{cases}$$

is a weak entropy solution of (2.1)–(2.2), (2.4).

Above we have written that the problem (2.1)–(2.2), (2.4) with $u_\ell < u_r$ possesses infinitely many solutions and that the solution u_1 does neither satisfy the entropy condition of Oleinik nor is an entropy solution. However, is u_2 the only solution satisfying (2.9) and (2.13)? The answer is affirmative but not easy to see, so we only cite the result (see [6]):

Theorem 2.10 *Let $f \in C^\infty(\mathbb{R})$ and $u_0 \in L^\infty(\mathbb{R})$. Then there exists at most one entropy solution of (2.1)–(2.2) satisfying the entropy condition (2.9).*

3 Traffic flow models

We present some simple traffic flow models. The first model has been already presented in Section 1:

(1) Lighthill-Whitham-Richards model:

$$\rho_t + (\rho v(\rho))_x = 0, \qquad v(\rho) = v_{\max}\left(1 - \frac{\rho}{\rho_{\max}}\right), \quad 0 \le \rho \le \rho_{\max}.$$

In Section 1 we have shown that this equation can be simplified by means of the transformation $u = 1 - 2\rho/\rho_{\max}$ to

$$u_t + \frac{1}{2}(u^2)_x = 0. \tag{3.1}$$

(2) Greenberg model: In this model it is assumed that the velocity of the vehicles can be very large for low densities:

$$\rho_t + (\rho v(\rho))_x = 0, \qquad v(\rho) = v_{\max} \ln \frac{\rho_{\max}}{\rho}, \quad 0 < \rho \le \rho_{\max}.$$

This implies

$$\rho_t - v_{\max}(\rho \ln \rho)_x = 0.$$

(3) Payne-Whitham model:

$$\rho_t + (\rho v)_x = 0, \qquad (\rho v)_t + (\rho v^2 + p(\rho))_x = 0.$$

This model mimics the flow of gas particles. In fact, the above equations are known as the Euler equations of gas dynamics with pressure $p(\rho) = a\rho^\gamma$, $a > 0$, $\gamma \ge 1$. The disadvantage of this model is that there may be solutions for which the velocity v is *negative* [3].

(4) Aw-Rascle model:

$$\rho_t + (\rho v)_x = 0, \qquad (\rho v + \rho p(\rho))_t + (\rho v^2 + \rho v p(\rho))_x = 0.$$

This model has been proposed as an improvement of the Payne-Whitham model [1]. It has been derived from microscopic models [2].

In the following, we will consider the Lighthill-Whitham-Richards model in some detail. More precisely, we want to study the influence of a temporal disturbance due to a traffic interruption (for instance, a traffic light). Suppose that the highway is initially filled with cars with uniform density $\overline{\rho}$ in the interval $(-\infty, 0)$, that there is a red light at $x = 0$, and that the highway is empty in $(0, \infty)$. We work with the transformed equation (3.1) and the uniform density $\overline{u} = 1 - 2\overline{\rho}/\rho_{\max}$. Clearly, there will be a tailback in front of the traffic light. At time $t = \omega$, the traffic light changes from red to green, and

the cars move from the left to the right. We want to know what happens with the tailback at time $t > \omega$.

First step: red phase ($0 \le t < \omega$). We solve the Burgers equation (3.1) for $x < 0$ with the initial function $u_0(x) = \overline{u}$, $x < 0$, and boundary condition $u(0,t) = -1$ (which models the red traffic light). The solution is (see Figure 3.1)

$$u(x,t) = \begin{cases} \overline{u} & : \ x < st \\ -1 & : \ x > st, \end{cases}$$

where $x < 0$, $0 < t < \omega$, and the shock speed s equals

$$s = \frac{u_\ell + u_r}{2} = \frac{\overline{u} - 1}{2}.$$

The solution for $x > 0$ is given by assumption by $u(x,t) = 1$, $x > 0$, $0 < t < \omega$.

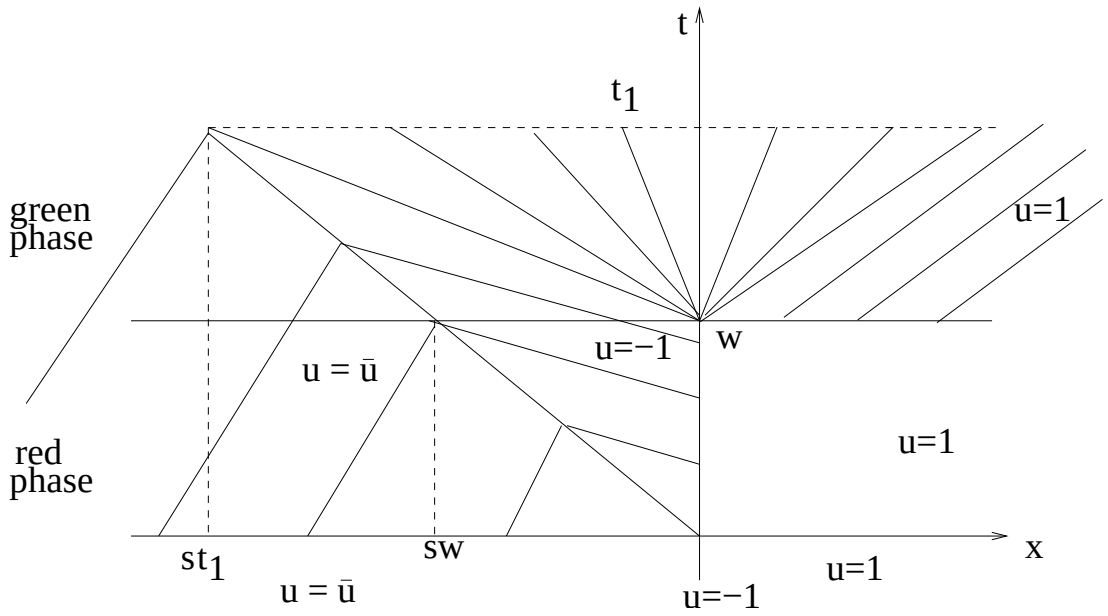

Figure 3.1: Characteristics for the traffic flow problem.

Second step: green phase ($t \ge \omega$). We solve the Burgers equation (3.1) in $\mathbb{R}$, with initial datum $u_0(x) = u(x,\omega)$. Since $u_\ell = \overline{u} > -1 = u_r$ we get a shock $\psi(t) = st$, $t > \omega$, with speed $s = (\overline{u} - 1)/2 < 0$. A rarefaction wave develops at $x = 0$, since $u_\ell = -1 < 1 = u_r$. The solution is given by

$$u(x,t) = \begin{cases} \overline{u} & : \ x < st, \\ -1 & : \ st \le x < \omega - t, \\ \frac{x}{t-\omega} & : \ \omega - t \le x \le t - \omega, \\ 1 & : \ x > t - \omega, \end{cases}$$

$x \in \mathbb{R}$, $t > \omega$. This solution makes sense as long as $st < \omega - t$ or, equivalently, $t < t_1 := \omega/(s+1) = 2\omega/(\overline{u}+1)$.

Third step: green phase ($t > t_1$). What happens with the shock for $t > t_1$? The shock speed is given by the generalized Ranking-Hugoniot condition (2.7):

$$\begin{aligned} s(t) \;=\; \psi'(t) \;&=\; \frac{1}{2}\left(u(\psi(t)+0,t) + u(\psi(t)-0,t)\right) \\ &=\; \frac{1}{2}\left(\frac{\psi(t)}{t-\omega} + \overline{u}\right), \qquad t > t_1. \end{aligned}$$

This is a linear ordinary differential equation with inital condition

$$\psi(t_1) = st_1 = \omega\frac{\overline{u}-1}{\overline{u}+1}.$$

The solution is

$$\psi(t) = \overline{u}(t-\omega) - \sqrt{t-\omega}\sqrt{\omega(1-\overline{u}^2)}, \qquad t \geq t_1.$$

Now there are two cases. If $\overline{u} \leq 0$, $\psi(t) \to -\infty$ as $t \to \infty$, i.e., there is a shock for all time and the shock moves into the negative x-direction with shock speed $\psi'(t) \to \overline{u}$ ($t \to \infty$). The velocity of the shock line is thus reduced from $s = (\overline{u}-1)/2$ to $\overline{u} \geq s$. Clearly, the discontinuity step at $\psi(t)$ goes to zero as $t \to \infty$. However, the drivers observe the shock even a long time after the traffic disturbance. This agrees with practical experience.

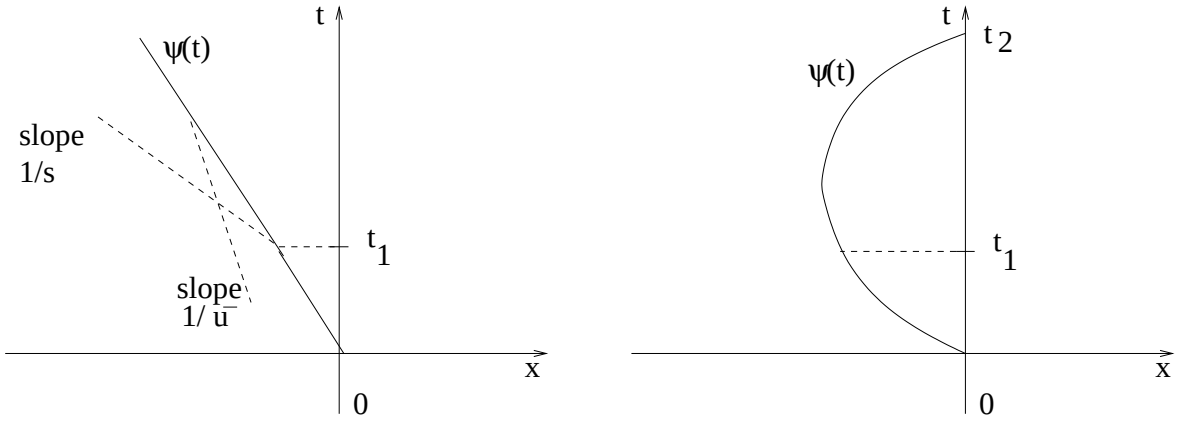

Figure 3.2: Shock curve $\psi(t)$ for $\overline{u} \leq 0$ (left) and $\overline{u} > 0$ (right).

In the other case, $\overline{u} > 0$, $\psi(t) \to \infty$ as $t \to \infty$, i.e., the shock line moves into the positive x-direction. Suppose that after the time $t = 2\omega$ the traffic light changes from green to red. How long should the green phase be to eliminate the shock, i.e., we need $t_2 \leq 2\omega$ where $\psi(t_2) = 0$. The equation $\psi(t_2) = 0$ has the (unique) solution $t_2 = \omega/\overline{u}^2$.

Thus, $t_2 \leq 2\omega$ is satisfied if and only if $\overline{u} \geq 1/\sqrt{2}$. The tailback in front of the traffic light will vanish during the green phase if and only if $\overline{u} \geq 1/\sqrt{2}$ or, in original density,

$$\rho \leq \rho_0 := \frac{\rho_{\max}}{2}\left(1 - \frac{1}{\sqrt{2}}\right) \approx 0.146\rho_{\max},$$

independently of the length of the green phase! Even for moderate vehicle density $\rho > \rho_0$, the tailback in front of the traffic light will become larger and larger as time increases.

4 Numerical approximation of scalar conservation laws

Before studying numerical methods for *nonlinear* scalar equations we start with a very simple *linear* equation:

$$u_t + au_x = 0, \qquad x \in \mathbb{R}, t > 0, \tag{4.1}$$

$$u(x,0) = u_0(x), \qquad x \in \mathbb{R}, \tag{4.2}$$

where $a > 0$. This problems has the explicit solution $u(x,t) = u_0(x - at)$ which is a weak solution (at least if u_0 is "smooth" enough).

We discretize the (x,t)-plane by the mesh (x_i, t_n) with

$$x_i = ih \quad (i \in \mathbb{Z}), \qquad t_n = nk \quad (n \in \mathbb{N}_0)$$

and $h, k > 0$. For simplicity of presentation we take a uniform mesh with h and k constant, but the discussed methods can be easily extended to non-uniform meshes. We are looking for finite difference approximations u_i^n to the solution $u(x_i, t_n)$ at the discrete grid points. The idea is to replace the partial derivatives in (4.1) by difference quotients. For example, (4.1) can be written by Taylor expansion as

$$\frac{u(x_i, t_{n+1}) - u(x_i, t_n)}{k} + \mathcal{O}(k) = -a\,\frac{u(x_{i+1}) - u(x_{i-1})}{2h} + \mathcal{O}(h^2), \tag{4.3}$$

which motivates the first numerical scheme:

Central scheme: Consider the approximation of (4.3)

$$\frac{u_i^{n+1} - u_i^n}{k} = -a\,\frac{u_{i+1}^n - u_{i-1}^n}{2h}, \qquad n \geq 0,\ i \in \mathbb{Z}.$$

We can write this scheme as

$$u_i^{n+1} = u_i^n - \frac{ak}{2h}\,(u_{i+1}^n - u_{i-1}^n). \tag{4.4}$$

As we can compute u_i^{n+1} from the data u_i^n explicitely, this is an *explicit* scheme. Another idea would be to use the scheme

$$\frac{u_i^{n+1} - u_i^n}{k} = -a \, \frac{u_{i+1}^{n+1} - u_{i-1}^{n+1}}{2h}$$

or, equivalently,

$$\frac{ak}{2h} u_{i+1}^{n+1} + u_i^{n+1} - \frac{ak}{2h} u_{i-1}^{n+1} = u_i^n.$$

This is an *implicit* scheme. In each time step, a linear system has to be solved. As for time-dependent hyerbolic equations, implicit schemes are rarely used, we consider in the following only explicit schemes.

In practice we must compute on a finite spatial domain, say $0 \le x \le Nh$, and we require appropriate boundary conditions at $x = 0$, $x = Nh$, respectively. For the above equation we choose *periodic* boundary conditions

$$u(0,t) = u(Nh,t), \qquad t > 0,$$

or, for the approximations u_i^n,

$$u_0^n = u_N^n, \qquad n \ge 0.$$

We can determine u_0^n and u_N^n using (4.4). In fact, setting $i = 0$ or $i = N$ in (4.4) would require to determine u_{-1}^n or u_{N+1}^n, We consider these points as artificial points with $u_{-1}^n = u_{N-1}^n$ and $u_N^n = u_0^N$, by the periodicity. Therefore, our central scheme reads as follows

$$\begin{aligned}
u_i^0 &= u_0(x_i), \qquad i = 0, \ldots, N, \\
u_i^{n+1} &= u_i^n - \frac{ak}{2h}(u_{i+1}^n - u_{i-1}^n), \qquad i = 1, \ldots, N-1, \\
u_0^{n+1} &= u_0^n - \frac{ak}{2h}(u_1^n - u_{N-1}^n), \\
u_N^{n+1} &= u_N^n - \frac{ak}{2h}(u_1^n - u_{N-1}^n).
\end{aligned}$$

Thus, if $u_0^n = u_N^n$ then $u_0^{n+1} = u_N^{n+1}$, and the periodicity is preserved. This scheme has the advantage that it is *mass-preserving*, i.e.

$$\sum_{i=0}^{N-1} u_i^n = \sum_{i=0}^{N-1} u_0(x_i), \qquad n \ge 0.$$

Indeed,

$$\begin{aligned}
\sum_{i=0}^{N-1} u_i^{n+1} &= \sum_{i=1}^{N-1} \left[u_i^n - \frac{ak}{2h}(u_{i+1}^n - u_{i-1}^n) \right] + u_0^n - \frac{ak}{2h}(u_1^n - u_{N-1}^n) \\
&= \sum_{i=0}^{N-1} u_i^n - \frac{ak}{2h} \left(\sum_{i=0}^{N-1} u_{i+1}^n - \sum_{i=1}^{N} u_{i-1}^n \right) \\
&= \sum_{i=0}^{N} u_i^n - \frac{ak}{2h}(u_N^n - u_0^n) \\
&= \sum_{i=0}^{N} u_i^n.
\end{aligned}$$

Figure 4.1 (first row, left) shows the numerical solution using the above central scheme for $a = 1$, $h = 0.01$, $N = 100$, $k = 0.001$, with initial data

$$u_0(x) = \sin(2\pi x), \qquad 0 \le x \le 1, \tag{4.5}$$

at time $t = 0$ (broken line) and $t = 0.25$ (solid line). The result is an approximation of $\sin(2\pi(x - 0.25))$. We see that the solution is oscillating. This can be improved by using an arithemetic average in the approximation of the time derivative and leads to the following scheme.

Lax-Friedrichs scheme. In this scheme the time derivative is approximated by

$$\frac{1}{k} \left(u(x, t + k) - \frac{1}{2}(u(x + h, t) + u(x - h, t)) \right),$$

i.e.

$$u_i^{n+1} = \frac{1}{2}(u_{i+1}^n + u_{i-1}^n) - \frac{ak}{2h}(u_{i+1}^n - u_{i-1}^n), \qquad i = 1, \ldots, N - 1. \tag{4.6}$$

The initial and boundary data are approximated by the same idea as for the central scheme. It is not difficult to check that the Lax-Friedrichs scheme is mass-preserving. Its numerical solution in Figure 4.1 (first row, right) with the same parameters as above shows that there are no oscillations, but now the solution is too smeared out. What happened?

We use the exact solution in the scheme (4.6) to compute the so-called truncation error

$$TE(x, t) = \frac{1}{k} \left(u(x, t + k) - \frac{1}{2}(u(x + h, t) + u(x - h, t)) \right) + \frac{a}{2h}(u(x + h, t) - u(x - h, t)).$$

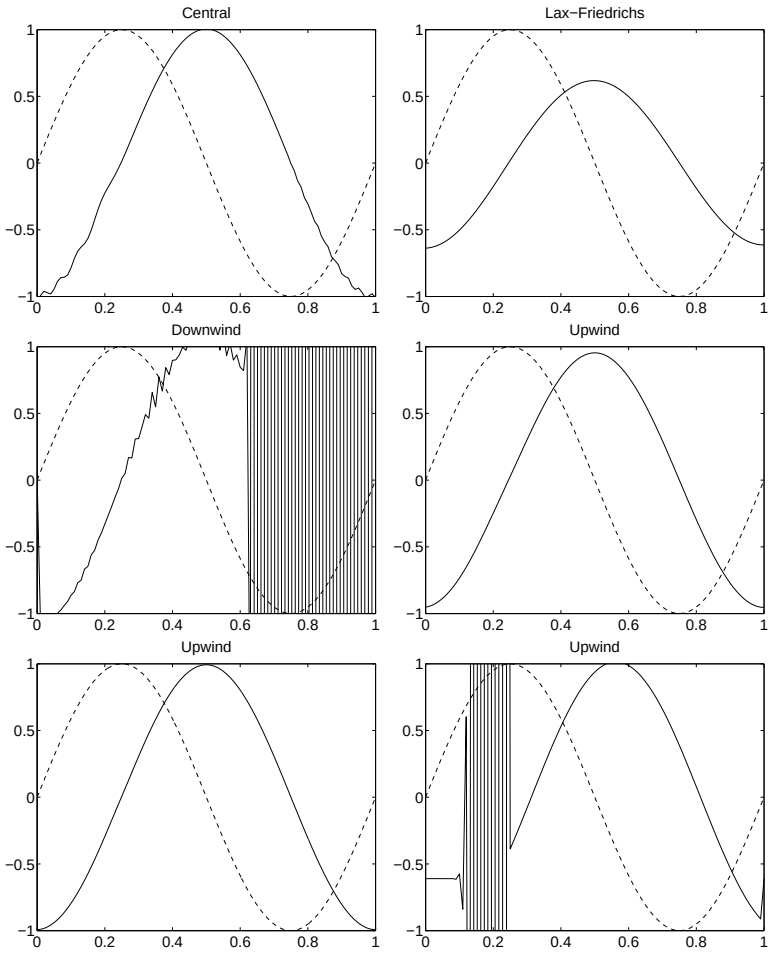

Figure 4.1: Various numerical schemes for (4.1) with $a = 1$, $h = 0.01$, $k = 0.001$ and smooth initial data (4.5). The numerical solution for $t = 0$ (broken line) and $t = 0.25$ (solid line) is shown. First row: central (left), Lax-Friedrichs (right); second row: downwind (left), upwind (right); last row: upwind but with $h = 0.002$ (left) and $k = 0.0025$ (right).

A Taylor expansion yields at (x, t)

$$\begin{aligned} TE &= \frac{1}{k}\left[\left(u + u_t k + \frac{1}{2}u_{tt}k^2 + O(k^3)\right) - \frac{1}{2}\left(2u + u_{xx}h^2 + O(h^4)\right)\right] \\ &\quad + \frac{a}{2h}(2u_x h + O(h^3)) \\ &= u_t + a u_x + \frac{1}{2}\left(u_{tt}k - u_{xx}\frac{h^2}{k}\right) + O(k^2) + O\Big(\frac{h^4}{k}\Big) + O(h^2). \end{aligned}$$

Since $u_{tt} = -a u_{xt} = a^2 u_{xx}$ and assuming that $k/h = \text{const.}$, we conclude

$$TE(x,t) = \frac{k}{2}\Big(a^2 - \Big(\frac{h}{k}\Big)^2\Big)u_{xx}(x,t) + O(h^2) = O(k). \tag{4.7}$$

This shows first that the Lax-Friedrichs scheme is a first-order method (as the truncation error satisfies $|TE(x,t)| \leq Ck$ for all (x,t)) and second that we approximate up to an error of the form ku_{xx}. Now, spatial second derivatives are modeling diffusion phenomena, and we expect the discrete solutions to be smeared out—justified by the numerical experiments. The numerical solution generated by the Lax-Friedrichs scheme can serve as an approximation of the advection-diffusion equation

$$u_t + au_x = -\frac{k}{2}\Big(a^2 - \Big(\frac{h}{k}\Big)^2\Big)u_{xx}, \qquad x \in \mathbb{R},\ t > 0.$$

For $h \to 0$ and $k \to 0$, the solutions of this modified equation converge (at least formally) to the solution of $u_t + au_x = 0$. This is related to the vanishing viscosity limit discussed in Section 3. The Lax-Friedrichs approximation becomes better and better for smaller $k > 0$. Moreover, the *artificial diffusion* (also called artificial viscosity) avoids oscillations.

Downwind scheme. The Lax-Friedrichs scheme gives accurate approximations only if k (or, equivalently, h if $k/h = \text{const.}$) is sufficiently small. One-sided finite difference approximations avoid too much artificial diffusion. Therefore, we choose the approximation

$$u_i^{n+1} = u_i^n - \frac{ak}{h}(u_{i+1}^n - u_i^n), \qquad i = 0, \ldots, N-1,$$

with initial and periodic boundary conditions analogously as above. Also this scheme is mass-preserving. The numerical solution shows that the scheme is unstable (Figure 4.1 (second row, left); same parameters as above). Why? The solution describes a "wave" from the left to the right. The spatial derivative at x_i, however, uses the information at x_{i+1} where the "wave" will go in the next time step. This does not make sense. In fact, the above scheme is useless. It would be more reasonable to use the information at x_{i-1} where the "wave" comes from. This is done in the following scheme.

Upwind scheme. This scheme reads as follows

$$u_i^{n+1} = u_i^n - \frac{ak}{h}(u_i^n - u_{i-1}^n), \qquad i = 1, \ldots, N. \tag{4.8}$$

Again, the scheme is mass-preserving. Its numerical solution with the same parameter values as in the previous schemes in Figure 4.1 (second row, right) shows the correct solution, no oscillations, but with artificial diffusion. In fact, the truncation error

$$TE(x,t) = \frac{1}{k}(u(x,t+k) - u(x,t)) + \frac{a}{h}(u(x,t) - u(x-h,t))$$

can be written as

$$TE(x,t) = \frac{ak}{2}\Big(a - \frac{h}{k}\Big)u_{xx} + O(h^2) + O(k^2). \tag{4.9}$$

The corresponding equation with artificial diffusion reads here:

$$u_t + au_x = -\frac{ah}{2}\Big(a - \frac{h}{k}\Big)u_{xx}. \tag{4.10}$$

For the values of a, k and h used here, the diffusion term is $0.0045u_{xx}$, whereas the corresponding term in the Lax-Friedrich scheme is $0.0495u_{xx}$. Thus, we expect upwind to be less diffusive than Lax-Friedrichs, as confirmed by the numerical experiments. Choosing $h > 0$ smaller, the diffusion becomes less apparent and for $h = 0.002$ the numerical solution is close to the exact solution (Figure 4.1 (last row, left)).

For small $k > 0$, we need a lot of time steps to compute the solution at a certain fixed time. Can we accelerate the computations by choosing k larger? Figure 4.1 (last row, right) shows the result for $h = 0.01$ and $k = 0.0025$ (a and u_0 are as above). Thus, the answer is no. Why? The modified equation (4.10) is well-posed only if the diffusion coefficient is non-negative:

$$-\frac{ah}{2}\Big(a - \frac{h}{k}\Big) \geq 0 \quad \Longleftrightarrow \quad \frac{ak}{h} \leq 1. \tag{4.11}$$

In the converse case we do not have diffusion but concentration. In the above situation we have $ak/h = 2.5 > 1$, and we expect the solution to break down after some time. The condition (4.11) is known as the Courant-Friedrich-Levy (CFL) condition. Strictly speaking, the CFL condition is not defined by (4.11) but equivalent to it, and we will identify the CFL condition and (4.11). This condition imposes a severe restriction on the choice of the time step; the more accurate the solution is computed (we mean: $h > 0$ small), the smaller $k > 0$ has to be chosen and the longer the computations take.

In Figure 4.2 we illustrate the described behavior using discontinuous initial data

$$u_0(x) = \begin{cases} 1 & : \quad 0 \leq x < 1/2 \\ 0 & : \quad 1/2 \leq x \leq 1 \end{cases} \tag{4.12}$$

and the parameters $a = 1$, $t = 0.25$, $k = 0.001$. We restrict the computational domain to $[0, 1]$. We do not choose periodic boundary conditions here, but inflow- and outflow-type conditions. In the traffic flow interpretation, the traffic is heavy in $[0, 1/2)$ and light in $[1/2, 1]$. So, at $x = 0$, cars are entering the domain and are leaving at $x = 1$. Hence, in the discrete formulation,

$$u_1^{n+1} = u_0^n \qquad \text{and} \qquad u_N^{n+1} = u_{N-1}^n, \qquad n \geq 0. \tag{4.13}$$

We observe again that the central scheme is oscillatory with damped oscillations for smaller k (Figure 4.2 (first row, left); $h = 0.01$); the Lax-Friedrichs scheme is quite diffusive but not oscillatory (Figure 4.2 (first row, right)); and the upwind scheme is less diffusive than the Lax-Friedrichs scheme (Figure 4.2 (last row, left)). Choosing the mesh

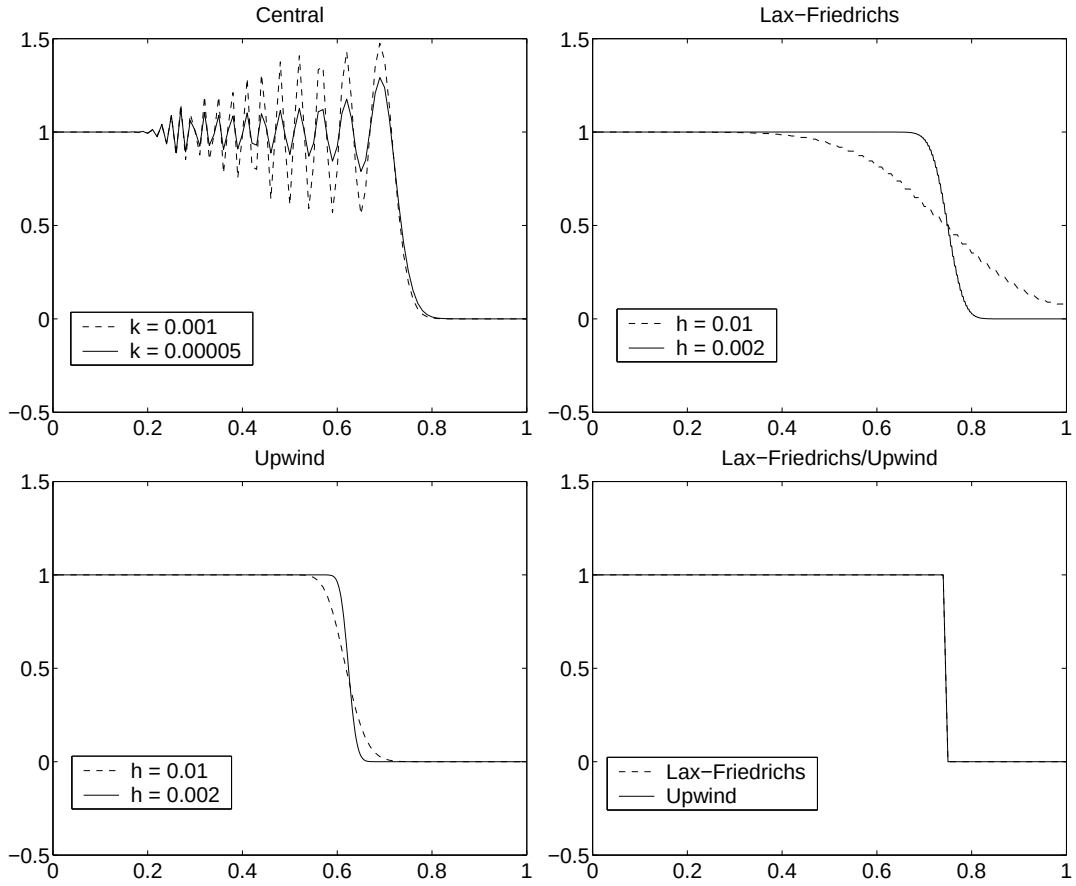

Figure 4.2: Various numerical schemes for (4.1) with $a = 1$ and discontinous data (4.12). First row, left: central; first row, right: Lax-Friedrichs; last row, left: upwind; last row, right: Lax-Friedrichs (broken line) and upwind (solid line) for $h = 0.001$, $k = 0.001$.

size $h = k = 0.01$, both schemes produce a solution which is very close to the exact solution (Figure 4.2 (last row, right)). This is clear since for this choice, $a - h/k = 0$ holds and thus, the artificial diffusion in (4.7) and (4.9) vanishes. All these schemes are able to compute the correct shock speed.

Summarizing the above results we observe that the central scheme tends to produce oscillations whereas the other diffusive schemes have usually too much artificial viscosity except for special mesh sizes.

The traffic flow models are nonlinear, so we want to study what can happen when we discretize nonlinear equations. We choose the scaled Lighthill-Whitham-Richards model (which is the same as the inviscid Burgers equation)

$$u_t + uu_x = 0, \qquad x \in \mathbb{R},\ t > 0, \tag{4.14}$$

$$u(x,0) = u_0(x), \qquad x \in \mathbb{R}, \tag{4.15}$$

with initial data (4.12). A "natural" generalization of the linear upwind scheme could be

$$u_i^{n+1} = u_i^n - \frac{k}{h} u_i^n (u_i^n - u_{i-1}^n), \qquad t \in \mathbb{Z},\ n \geq 0.$$

Since $u_i^0 = 0$ if $i \geq N/2$ and $u_i^0 - u_{i-1}^0 = 0$ for $i < N/2$, $u_i^1 = u_i^0$ for all i. This happens in every time step and so $u_i^n = u_i^0$ for all i. As the grid is refined, the numerical solution converges to the function $u(x,t) = u_0(x)$. This is not a weak solution of (4.14)–(4.15)!

One might think that the upwind scheme

$$u_i^{n+1} = u_i^n - \frac{k}{h} u_{i-1}^n (u_i^n - u_{i-1}^n), \qquad i \in \mathbb{Z},\ n \geq 0, \tag{4.16}$$

gives better results since here we use the information from the left where the "wave" is coming from. The numerical solution of this scheme (with boundary conditions (4.13) and $k = 0.001$, $t = 0.5$) is depicted in Figure 4.3 (left). For smaller mesh size, the numerical solution converges nicely to a function of type $u_0(x - at)$. The exact solution of (4.14)–(4.15), (4.12) is

$$u(x,t) = \begin{cases} 1 & : \quad x < st \\ 0 & : \quad x > st \end{cases}$$

with $s = \frac{1}{2}(u_\ell + u_r) = \frac{1}{2}$. At $t = \frac{1}{2}$, the discontinuity should be at $x = \frac{3}{4}$. Thus, the numerical solution propagates with the wrong speed!

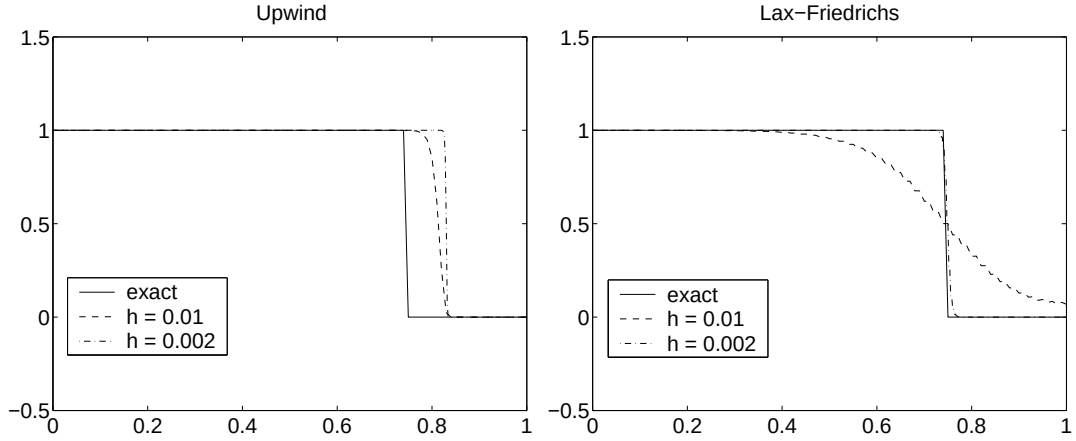

Figure 4.3: Exact and numerical solutions for the inviscid Burger equation using the upwind scheme (4.16) (left) and the Lax-Friedrichs scheme (4.17) (right).

A better behavior is given by the Lax-Friedrichs scheme

$$u_i^{n+1} = \frac{1}{2}(u_{i+1}^n + u_{i-1}^n) - \frac{k}{4h}\left((u_{i+1}^n)^2 - (u_{i-1}^n)^2\right), \qquad i \in \mathbb{Z},\ n \geq 0. \tag{4.17}$$

From Figure 4.3 (right) we see that the scheme is non-oscillatory and the shock speed is correct.

What is the reason for the different shock speeds? The upwind scheme (4.16) is a discretization of the quasilinear equation

$$u_t + uu_x = 0,$$

whereas the scheme (4.17) is an approximation of the equation in conservation form

$$u_t + \left(\frac{u^2}{2}\right)_x = 0.$$

For smooth solutions both equations are the same, but we know from Section 2 (see, for instance, Example 2.8) that this may not be true for weak solutions.

In the following we consider only numerical methods being in *conservation form*, meaning that the scheme is of the form

$$u_i^{n+1} = u_i^n - \frac{k}{h}[F(u_{i-p}^n, \ldots, u_{i+q}^n) - F(u_{i-1-p}^n, \ldots, u_{i-1+q}^n)]$$

for some function F of $p+q+1$ arguments. We call F the *numerical flux function*. The simplest case is for $p = 0$ and $q = 1$, where

$$u_i^{n+1} = u_i^n - \frac{k}{h}[F(u_i^n, u_{i+1}^n) - F(u_{i-1}^n, u_i^n)]. \tag{4.18}$$

This expression can be interpreted as a cell average. More precisely, we know that the weak solution of

$$u_t + f(u)_x = 0, \qquad x \in \mathbb{R},\ t > 0, \tag{4.19}$$

satisfies the integral form

$$\begin{aligned} \frac{1}{h}\int_{x_{i-1/2}}^{x_{i+1/2}} u(x, t_{n+1})\,dx &= \frac{1}{h}\int_{x_{i-1/2}}^{x_{i+1/2}} u(x, t_n)\,dx \\ &\quad - \frac{k}{h}\left[\frac{1}{k}\int_{t_n}^{t_{n+1}} f(u(x_{i+1/2}, t))\,dt - \frac{1}{k}\int_{t_n}^{t_{n+1}} f(u(x_{i-1/2}, t))\,dt\right], \end{aligned} \tag{4.20}$$

where $x_{i\pm1/2} = (i \pm 1/2)h$ denotes the cell middle points (see Figure 4.4). Interpretating u_i^n as approximations of the cell averages,

$$u_i^n \sim \frac{1}{h}\int_{x_{i-1/2}}^{x_{i+1/2}} u(x, t_n)\,dx,$$

and $F(u_i^n, u_{i+1}^n)$ as approximations of the average flux through $x_{i+1/2}$ over the time interval (t_n, t_{n+1}),

$$F(u_i^n, u_{i+1}^n) \sim \frac{1}{k}\int_{t_n}^{t_{n+1}} f(u(x_{i+1/2}, t))\,dt,$$

we obtain the approximation (4.18) from (4.20).

We give now some examples of numerical methods in conservation form:

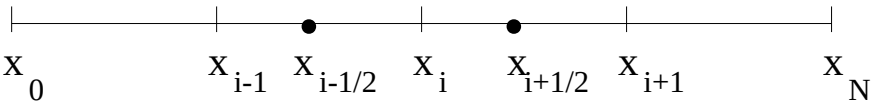

Figure 4.4: The spatial mesh.

Example 4.1

(1) Lax-Friedrichs scheme:

$$u_i^{n+1} = \frac{1}{2}(u_{i+1}^n + u_{i-1}^n) - \frac{k}{2h}(f(u_{i+1}^n) - f(u_{i-1}^n)).$$

This method can be written in the conservation form (4.18) by taking

$$F(u_i^n, u_{i+1}^n) = \frac{h}{2k}(u_i - u_{i+1}) + \frac{1}{2}(f(u_i) + f(u_{i+1})).$$

It can be proved that this scheme is a first-order method (i.e., the truncation error TE satisfies $|TE| = O(k)$ as $k \to 0$).

(2) Lax-Wendroff scheme:

$$\begin{aligned} u_i^{n+1} &= u_i^n - \frac{k}{2h}(f(u_{i+1}^n) - f(u_{i-1}^n)) \\ &\quad + \frac{k^2}{2h^2}[f'(u_{i+1/2}^n)(f(u_{i+1}^n) - f(u_i^n)) - f'(u_{i-1/2}^n)(f(u_i^n) - f(u_{i-1}^n))], \end{aligned}$$

where $u_{i\pm1/2}^n = \frac{1}{2}(u_i^n + u_{i\pm1/2}^n)$. This is a second-order method (i.e. $|TE| = O(k^2)$ as $k \to 0$). It has the disadvantage that it requires evaluating f' in two points at each time step which is expensive when we deal with systems of conservation laws (and f' is the Jacobi matrix). This is avoided in the following schemes.

(3) Richtmyer two-step Lax-Wendroff scheme:

$$\begin{aligned} u_i^* &= \frac{1}{2}(u_i^n + u_{i+1}^n) - \frac{k}{h}[f(u_{i+1}^n) - f(u_i^n)], \\ u_i^{n+1} &= u_i^n - \frac{k}{h}[f(u_i^*) - f(u_{i-1}^*)]. \end{aligned}$$

This is a second-order method. Notice that the derivation of the local truncation error $TE(x,t)$ needs smooth solutions, so all these second-order methods are of second order for *smooth* solutions. The methods are usually only of first order around shocks.

(4) Mac-Cornack scheme:

$$\begin{aligned} u_i^* &= u_i^n - \frac{k}{h}[f(u_{i+1}^n) - f(u_i^n)], \\ u_i^{n+1} &= \frac{1}{2}(u_i^n + u_i^*) - \frac{k}{h}[f(u_i^*) - f(u_{i-1}^*)]. \end{aligned}$$

This scheme uses first forward differencing and then backward differencing. It is also a second-order method. Notice that the schemes (2)–(4) reduce to the Lax-Wendroff method if f is linear.

All the described schemes in Example 4.1 yield numerical solutions which converge to a weak solution of (4.19) if the mesh discretization parameters h and k tend to zero. In order to formulate this result more generally we need the following definitions. From now on, we assume that $f : \mathbb{R}^n \to \mathbb{R}^n$ is a vector-valued function, i.e., we consider *systems* of conservation laws (4.19).

Definition 4.2 *(1) A difference scheme of the form*

$$u_i^{n+1} = u_i^n - \frac{k}{h}[F(u_{i-p}^n, \ldots, u_{i+q}^n) - F(u_{i-1-p}^n, \ldots, u_{i-1+q}^n)]$$

for some function $F : (\mathbb{R}^n)^{p+q+1} \to \mathbb{R}^n$ is called conservative.

(2) A conservative scheme is called consistent *if F is locally Lipschitz continuous and*

$$F(u, \ldots, u) = f(u) \quad \forall\, u \in \mathbb{R}.$$

(3) The total variation *$TV(v)$ of a function $v : \mathbb{R} \to \mathbb{R}^n$ is defined by*

$$TV(v) = \sup \sum_{i=1}^{N} |v(\xi_i) - v(\xi_{i-1})|,$$

where the supremum is taken over all subdivisions $-\infty = \xi_0 < \xi_1 < \ldots < \xi_n = \infty$ of the real line.

Notice that for the total variation to be finite v must approach constant values as $x \to \pm\infty$. For differentiable v the definition reduces to

$$TV(v) = \int_{\mathbb{R}} |v'(x)|\, dx.$$

Theorem 4.3 (Lax-Wendroff) *Let $u_j(x,t)$ be a numerical solution computed with a consistent and conservative method on a mesh with mesh size h_j and time step k_j, with $h_j, k_j \to 0$ as $j \to \infty$. (The function u_j can be, for instance, the constant extension of u_i^n in the cells.) Assume that there exists a function $u(x,t)$ such that*

(1) for all $a, b \in \mathbb{R}$, $T > 0$,

$$\int_0^T \int_a^b |u_j(x,t) - u(x,t)|\, dxdt \to 0 \qquad \text{as } j \to \infty,$$

(2) for all $T > 0$ there is a number $K > 0$ such that

$$TV(u_j(\cdot,t)) \le K \qquad \forall\, 0 \le t \le T,\ j \in \mathbb{N}.$$

Then $u(x,t)$ is a weak solution of (4.19).

For the proof we refer to [5, Sec. 12]. Theorem 4.3 does not guarantee that weak solutions obtained in this way satisfy the entropy condition. This is true under the following additional condition.

Theorem 4.4 *Let (η, ψ) be an entropy-entropy flux pair such that $\eta''(u) > 0$ and $\eta'(u)$ $\operatorname{div} f(u) = \operatorname{div} \psi(u)$ for all $u \in \mathbb{R}^n$. Furthermore, let Ψ be a numerical flux function consistent with ψ in the sense of Definition 4.2 (2). Let the assumptions of Theorem 4.3 hold and, additionally,*

$$\eta(u_i^{n+1}) \le \eta(u_i^n) - \frac{k}{h}[\Psi(u_{i-p}^n, \ldots, u_{i+q}^n) - \Psi(u_{i-1-p}^n, \ldots, u_{i-1+q}^n)]$$

for all i, n. Then $u(x,t)$ (obtained in Theorem 4.3) satisfies the entropy inequality (2.13).

Again, we refer to [5, Sec. 12] for a proof.

5 The Gudonov method

In Section 4 we have seen that a nonlinear conservation law (or a system of conservation laws) can be numerically approximated by the Lax-Friedrichs scheme. For the linear advection equation (4.1) we have also seen that the Lax-Friedrichs scheme is generally more dissipative than the upwind method and gives less accurate solutions. In the scalar case, a natural generalization of the upwind scheme (4.8) is

$$u_i^{n+1} = u_i^n - \frac{k}{h}[F(u_i^n, u_{i+1}^n) - F(u_{i-1}^n, u_i^n)] \tag{5.1}$$

with

$$F(v,w) = \begin{cases} f(v) & : \ (f(v) - f(w))/(v-w) \ge 0 \\ f(w) & : \ (f(v) - f(w))/(v-w) < 0. \end{cases}$$

For linear equations, $F(v,w) = f(v)$ and (5.1) reduces to (4.8). However, the above scheme may not give the correct approximation. For instance, let $f(u) = u^2/2$ and choose the initial data

$$u_i^0 = \begin{cases} -1 & : \quad i \le 0 \\ +1 & : \quad i > 0. \end{cases}$$

Since $F(u_i^0, u_{i+1}^0)$ and $F(u_{i-1}^0, u_i^0)$ are either equal to $f(-1)$ or $f(1)$ and since $f(-1) = f(1)$, we obtain $u_i^1 = u_i^0$ for all i and hence $u_i^n = u_i^0$ for all i. This is not the correct discrete solution.

In this section we derive a conservative and consistent generalization of the upwind scheme which avoids the above problem, the so-called *Gudonov scheme*. Let f be a convex C^2 function. The idea of the method is to approximate the solution $u(x,t_n)$ of the conservation law (scalar or system)

$$u_t + f(u)_x = 0, \qquad x \in \mathbb{R},\ t > 0,$$

by a piecewise constant function $\widetilde{u}^n(x,t_n)$ and to determine the approximate solution $\widetilde{u}^n(x,t)$ by solving the Riemann problem in the interval $t \in [t_n, t_{n+1}]$. After obtaining this solution, we define the approximate solution u_i^{n+1} at time t_{n+1} by averaging this exact solution at time t_{n+1}:

$$u_i^{n+1} = \frac{1}{h}\int_{x_{i-1/2}}^{x_{i+1/2}} \widetilde{u}^n(x,t_{n+1})\,dx, \tag{5.2}$$

where $x_{i\pm1/2} = (i \pm 1/2)h$. These values are then used to define the new piecewise constant data $\widetilde{u}^{n+1}(x,t_{n+1})$ by

$$\widetilde{u}^{n+1}(x,t_{n+1}) = u_i^{n+1} \qquad \text{if} \quad x_{i-1/2} \le x < x_{i+1/2},$$

and the process repeats.

In practice, this algorithm is considerably simplified since the above integral can be computed explicitely. Since $\widetilde{u}^n$ is assumed to be the exact weak solution, it satisfies the integral formulation (2.3) divided by h:

$$\begin{aligned} &\frac{1}{h}\int_{x_{i-1/2}}^{x_{i+1/2}} \widetilde{u}^n(x,t_{n+1})\,dx \\ &= \frac{1}{h}\int_{x_{i-1/2}}^{x_{i+1/2}} \widetilde{u}^n(x,t_n)\,dx \\ &\quad - \frac{k}{h}\left[\frac{1}{k}\int_{t_n}^{t_{n+1}} f(\widetilde{u}^n(x_{i+1/2},t))\,dt - \frac{1}{k}\int_{t_n}^{t_{n+1}} f(\widetilde{u}^n(x_{i-1/2},t))\,dt\right]. \end{aligned}$$

From (5.2) follows

$$u_i^{n+1} = u_i^n - \frac{k}{h}\left[F(u_i^n, u_{i+1}^n) - F(u_{i-1}^n, u_i^n)\right], \tag{5.3}$$

where the numerical flux function F is given by

$$F(u_i^n, u_{i+1}^n) = \frac{1}{k} \int_{t_n}^{t_{n+1}} f(\widetilde{u}^n(x_{i+1/2}, t))\, dt.$$

Thus, the Gudonov scheme is conservative (see Definition 4.2). The function $\widetilde{u}^n$ is constant on the line $x = x_{i+1/2}$, $t_n \le t \le t_{n+1}$ (see Figure 5.1). We denote this value by $u^*(u_i^n, u_{i+1}^n)$.

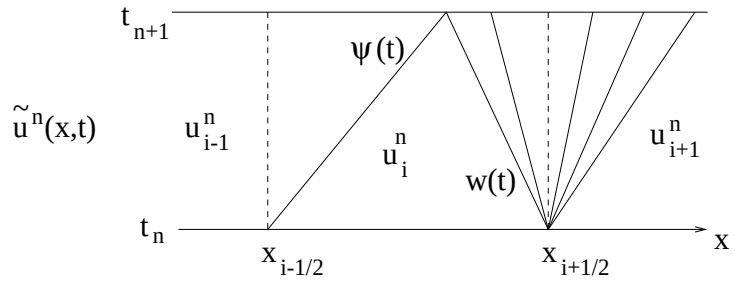

Figure 5.1: Illustration for the Gudonov scheme. There is a shock through $x_{i-1/2}$ and a rarefaction wave starting at $x_{i+1/2}$.

Then the flux reduces to

$$F(u_i^n, u_{i+1}^n) = f(u^*(u_i^n, u_{i+1}^n))$$

and the Gudonov scheme becomes

$$u_i^{n+1} = u_i^n - \frac{k}{h}[f(u^*(u_i^n, u_{i+1}^n)) - f(u^*(u_{i-1}^n, u_i^n))].$$

The scheme is consistent (see Definition 4.2) since $F(u_i^n, u_i^n) = f(u_i^n)$ and f is assumed to be smooth.

There are two questions remaining:

- For large $t - t_n$, the solution may not remain constant at $x_{i+1/2}$ because of the effects of waves arising from neighboring Riemann problems. How large can $k = t_{n+1} - t_n$ be chosen?
- How can we determine u^* from u_i^n, u_{i+1}^n?

We answer the first question. Assume the situation of Figure 5.1, i.e., let $\psi(t)$ be the shock line through $x_{i-1/2}$ and let $w(t)$ be the left end of the rarefaction wave starting at $x_{i+1/2}$. The time t_{n+1} is determined by the requirement $\psi(t_{n+1}) \le w(t_{n+1})$. Since

$$\psi(t) = x_{i-1/2} + s(t - t_n) \qquad \text{with} \quad s = \frac{f(u_{i+1}^n) - f(u_i^n)}{u_{i+1}^n - u_i^n}$$

and

$$w(t) = x_{i+1/2} + f'(u_i^n)(t - t_n),$$

this yields

$$h = x_{i+1/2} - x_{x-1/2} \geq (s - f'(u_i^n))(t_{n+1} - t_n) = (s - f'(u_i^n))k. \tag{5.4}$$

As f is assumed to be convex, s lies between $f'(u_i^n)$ and $f'(u_{i+1}^n)$, i.e.

$$|s| \leq \max\{|f'(u_i^n)|, |f'(u_{i+1}^n)|\}.$$

Thus, if

$$\nu := \sup_{i,n} \left| \frac{f'(u_i^n)k}{h} \right| \leq \frac{1}{2} \tag{5.5}$$

we infer

$$s - f'(u_{i+1}^n) \leq |s| + |f'(u_i^n)| \leq 2 \sup_{i,n} |f'(u_i^n)| \leq \frac{h}{k},$$

and (5.4) is satisfied. The condition (5.5) ensures that the shock and the rarefaction wave do not interact in the mesh cell $[x_{i-1/2}, x_{i+1/2}] \times [t_n, t_{n+1})$. We obtain the same condition (5.5) if there is a rarefaction wave at $x_{i-1/2}$ and a shock at $x_{i+1/2}$ or if there are two shocks at $x_{i\pm 1/2}$ since the wave speeds are always bounded by $\sup |f'(u_i^n)|$.

In fact, we can allow the waves to interact during the time step, provided the interaction is entirely contained within a mesh cell. This leads to the condition $2 \sup |f'(u_i^n)| \leq 2h/k$ or

$$\nu = \sup_{i,n} \left| f'(u_i^n) \frac{k}{h} \right| \leq 1. \tag{5.6}$$

This condition can be interpreted as a generalization of the CFL condition (4.11) for linear conservation laws. In the case of *systems* of conservation laws we replace (5.6) by

$$\sup_{i,n,p} \left| \lambda_p(u_i^n) \frac{k}{h} \right| \leq 1,$$

where $\lambda_p(u_i^n)$ are the eigenvalues of the Jacobian $f'(u_i^n)$. This answers the first question.

Concerning the second question, we need to solve the Riemann problem to determine $u^*(u_i^n, u_{i+1}^n)$. For *systems* of conservation laws, this may be expensive. Notice however, that most of the structure of the Riemann solver is not used in the Gudonov scheme and therefore, approximate Riemann solvers have been devised to improve the efficiency of the Gudonov method. We do not describe these approximate solvers but refer to [5, Sec. 14.2]. For *scalar* conservation laws, we can determine u^* easily from the sign of $f'(u_i^n)$ and $f'(u_{i+1}^n)$. Indeed, we consider the following four cases:

(1) $f'(u_i^n) \geq 0$ and $f'(u_{i+1}^n) \geq 0$: In this case there is a rarefaction wave starting at $x_{i+1/2}$, and from Figure 5.2 (a) we see that $u^* = u_i^n$.

(2) $f'(u_i^n) < 0$ and $f'(u_{i+1}^n) < 0$: Again, there is a rarefaction wave starting at $x_{i+1/2}$ but now $u^* = u_{i+1}^n$ (see Figure 5.2 (b)).

(3) $f'(u_i^n) \geq 0$ and $f'(u_{i+1}^n) < 0$: There is a shock through $x_{i+1/2}$ and (Figure 5.2 (c))

$$u^* = \begin{cases} u_i^n & : \ s \geq 0 \\ u_{i+1}^n & : \ s < 0. \end{cases}$$

(4) $f'(u_i^n) < 0$ and $f'(u_{i+1}^n) \geq 0$: There is a rarefaction wave starting at $x_{i+1/2}$ and u^* is the unique solution of $f'(u^*) = 0$ (since f is convex). As the wave speed passes through zero within the wave it is called *transonic rarefaction wave* (Figure 5.2 (d)). The value u^* is called *sonic point*.

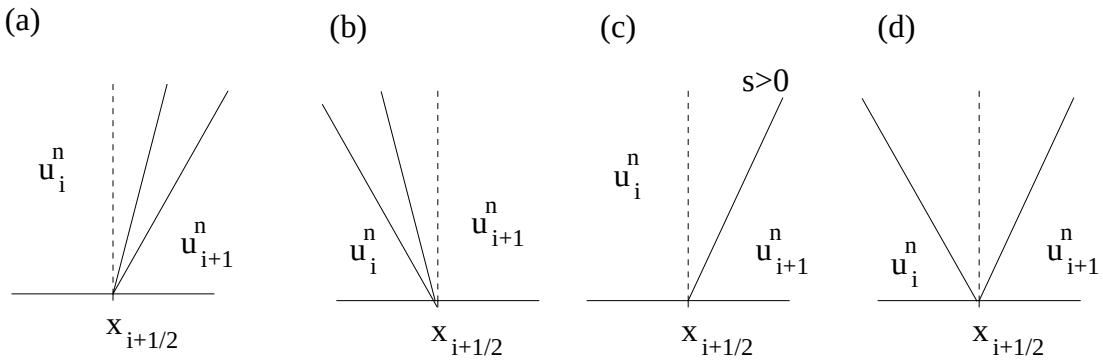

Figure 5.2: Computation of u^*.

The resulting flux function can be written in the simplified form

$$F(u_i^n, u_{i+1}^n) = \begin{cases} \min\limits_{u_i^n \leq u \leq u_{i+1}^n} f(u) & : \ u_i^n \leq u_{i+1}^n \\ \max\limits_{u_{i+1}^n \leq u \leq u_i^n} f(u) & : \ u_i^n > u_{i+1}^n. \end{cases}$$

Surprisingly, this expression also holds for general conservation laws, even non-convex ones, and gives the correct Gudonov flux corresponding to the weak solution satisfying the entropy condition (2.9) of Oleinik.

Example 5.1 For $f(u) = au$ $(a > 0)$ the flux function becomes

$$F(u_i^n, u_{i+1}^n) = au_i^n,$$

and hence, from (5.3), the Gudonov scheme is equal to the upwind scheme for linear equations (see Section 4),

$$u_i^{n+1} = u_i^n - \frac{ak}{h}(u_i^n - u_i^{n+1}).$$

In this sense, the Gudonov method is a generalization of the upwind scheme to nonlinear equations. □

We summarize the Gudonov scheme for scalar conservation laws:

- Initialize
$$u_i^0 = \frac{1}{h}\int_{x_{i-1/2}}^{x_{i+1/2}} u_0(x)\,dx.$$

- For all i, n do:
  if $f'(u_i^n) \geq 0$ and $f'(u_{i+1}^n) \geq 0$ then $u_i^* = u_i^n$;
  if $f'(u_i^n) < 0$ and $f'(u_{i+1}^n) < 0$ then $u_i^* = u_{i+1}^n$;
  if $f'(u_i^n) \geq 0$ and $f'(u_{i+1}^n) < 0$ then $u_i^* = u_i^n$ (if $s \geq 0$) or $u_i^* = u_{i+1}^n$ (if $s < 0$);
  if $f'(u_i^n) < 0$ and $f'(u_{i+1}^n) \geq 0$ then u_i^* is the unique solution of $f'(u_i^*) = 0$.

- Set
$$u_i^{n+1} = u_i^n - \frac{k}{h}[f(u_i^*) - f(u_{i-1}^*)].$$

References

[1] A. Aw and M. Rascle: Resurrection of "second order" models of traffic flow. SIAM J. Appl. Math. **60** (2000), 916-938.

[2] A. Aw, A. Klar, T. Materne, and M. Rascle: Derivation of continuum traffic flow models from microscopic follow-the-leader models. Submitted for publication, 2002.

[3] C. Daganzo: Requiem for second-order fluid approximation to traffic flow. Transport. Res. B **29** (1995), 277-286.

[4] M. Hanke-Bourgeois: *Grundlagen der Numerischen Mathematik und des Wissenschaftlichen Rechnens.* Teubner, Stuttgart, 2002.

[5] R. LeVeque: *Numerical Methods for Conservation Laws.* Birkhuser, Basel, 1990.

[6] G. Warnecke: *Analytische Methoden in der Theorie der Erhaltungsgleichungen.* Teubner, Stuttgart 1999.